

Record-breaking extremes in a warming climate

Erich M. Fischer ® ¹⊠, Margot Bador², Raphaël Huser³, Elizabeth J. Kendon ® ^{4,5}, Alexander Robinson ® ⁶ & Sebastian Sippel ® ⁷

Abstract

Numerous weather and climate extremes have broken long-standing observed records. These record-breaking (or record-shattering if the margin is large) events have substantial socioeconomic impacts and pose adaptation and planning challenges. In this Review, we assess observed and projected changes in record-breaking climate extremes. Record occurrence can be understood with statistical considerations, and their changes quantified as the record ratio – the observed frequency of record events relative to a stationary climate. Many climate variables have witnessed changes in their record-breaking frequency. For example, all-time daily hot records on land are more than four times higher in 2016–2024 than expected without climate change, and all-time cold records two times lower; similarly, daily maximum precipitation records and monthly dryness records are more than 40% and 10% higher, respectively. In the future, slowing the rate of warming reduces record ratios, highlighting the benefits of mitigation. For instance, by the end of the century, multimodel mean record hot events are projected to be 15.7 more likely than in a stationary climate under SSP3-7.0, but only ~2.9 and ~1.8 more likely for SSP1-2.6 and SSP1-1.9, respectively, lower than those observed today. New record cold will become virtually non-existent under all emission scenarios. Among others, records have also been broken for ice loss, sea ice and ocean heat content, but quantifying record statistics is challenged by data availability, duration and quality. Addressing these data challenges and developing statistical methods to account for multivariate records are research priorities.

Sections

Introduction

Record statistics

Hot and cold records

Hydrological records

Record behaviour across the climate system

Anticipating record events for adaptation

Summary and future perspectives

¹Institute for Atmospheric and Climate Science, ETH Zurich, Zurich, Switzerland. ²CECI CNRS/Cerfacs, Université de Toulouse, Toulouse, France. ³CEMSE Division, King Abdullah University of Science and Technology, Thuwal, Saudi Arabia. ⁴Met Office Hadley Centre, Exeter, UK. ⁵School of Geographical Sciences, University of Bristol, Bristol, UK. ⁶Alfred Wegener Institute, Helmholtz Centre for Polar and Marine Research, Potsdam, Germany. ⁷Institute for Meteorology, Leipzig University, Leipzig, Germany. ⊠e-mail: erich.fischer@env.ethz.ch

Introduction

Numerous weather and climate extremes have reached intensities that are unprecedented in the observational period. These so-called record-breaking events span many aspects of the climate system, perhaps most prominent for extreme heat. For instance, hot extremes in the Pacific Northwest in June and July 2021 (refs. 1-4), multimonth heat in Siberia in 2020 (refs. 5,6), large parts of China in summer 2022 (refs. 7.8) and the UK in summer 2022 (the first temperature >40 °C)⁹ shattered all-time observed records. Many of the largest record margins occurred in 2021-2024, a period of rapidly increasing global mean temperatures, but other events breaking records by the largest normalized margins include the 2003 European heatwave and the 2010 heatwave in Western Russia¹⁰⁻¹³ (Fig. 1). Likewise, several rainfall events have broken records by large margins, including over Australia in February and March 2022 (ref. 14), monsoon rainfall in Pakistan in August 2022 (refs. 15-17) and across Germany, Belgium and the Netherlands in July 2021 (ref. 18) (Supplementary Fig. 2).

Many of these record-breaking events had severe impacts on society, ecosystems and economies. For instance, the 2003 heatwave in western Europe led to about 70,000 heat-related deaths across Europe¹⁹, crop loss, challenges to energy demand and supply and wildfires²⁰; the 2021 Pacific Northwest heatwave had similar impacts⁴. Record-breaking heavy precipitation events also have substantial impacts, including fatalities as witnessed in Pakistan in 2010 (ref. 21), northwestern Germany in 2021 (ref. 18) and near Valencia in 2024. Of course, not all events have societal impact given their occurrence over sparsely population regions, as for record rainfall intensity at a rainfall gauge in Northern Italy in 2021 (ref. 22) or the record-breaking spring heat anomaly in Antarctica during 2022 (ref. 23).

The very large number of record-breaking events across the climate system is remarkable. Indeed, in a stationary climate, records are expected to become rarer the longer a measurement series. However, as the climate is non-stationary and rapidly warming, record hot events have been declining slower since the 1980s and even increasing since the late 1990s over land and oceans $^{24-27}$. Many of these events since 2000 were even record-shattering heat events $^{28,29}-a$ subgroup of record-breaking events wherein the existing record is broken by a large margin, typically more than 1 standard deviation of annual maxima in the reference period. Record-breaking events have also been commonplace in heavy precipitation and dryness $^{30-32}$ and minima for Arctic and Antarctic sea ice extent and volumes of glacier and ice sheets.

In this Review, we assess the current understanding of record-breaking events in a warming climate. We begin with a theoretical consideration, examining the statistics of record behaviour and its dependence on the underlying changes in the distribution of different variables. We follow by quantifying past and projected future changes in different types of record-breaking events, including hot and cold, wet and dry events, and those in other climatic variables. Next, we discuss the relevance of different record-breaking event characteristics for impacts on society, economy and ecosystems. We end with a discussion of knowledge gaps and recommendations for future research to address key challenges.

Record statistics

Statistically defining the occurrence or likelihood of record events have long been of interest. For example, the so-called 1990 Hansen bet $^{\rm 33}$ quantified the likelihood that one of the next three years would be the hottest in 100 years globally $^{\rm 34}$. In a stationary climate (and assuming no temporal autocorrelation), the odds for such an event were around 5%

(ref. 33), but under the more realistic assumption of non-stationarity owing to forced climate change and temporal autocorrelation, the odds could be as high as 75% (ref. 33). The global temperature record was broken in 1990. Since then, the statistics behind record events have expanded in climate extreme research. Key theoretical and statistical considerations of record-breaking events are now discussed.

Record occurrence probability and record margins

By definition, records are supposed to be rare events, at least under stationary conditions. Thus, their statistical properties are closely linked to the statistics of extremes $^{35-37}$. For a univariate time series with a sequence of n consecutive observations $X_1, ..., X_n$, the last observation is said to be a record if it exceeds all past observations. That is, if:

$$X_n > \max(X_1, ..., X_{n-1}).$$
 (1)

If all observations are independent and identically distributed (i.i.d.) random variables, any of them is equally likely to be the sample maximum. Therefore, the probability of a record event in equation (1) at time step n is simply 1/n, irrespective of the distribution of X_t . The record probability thus decreases at a fast rate with increasing sample size over time (n). Moreover, the expected number of records up to time n is approximately $y + \log(n)$ for large n, with $y \approx 0.577$, the Euler–Mascheroni constant. Hence, a given i.i.d. time series of n = 100 samples would be expected to contain on average about $y + \log(100) \approx 5.18$ record events. This expected record number corresponds to adding the sum of the odds for each time step, that is:

$$\sum_{i=1}^{n=100} \frac{1}{i} = \frac{1}{1} + \frac{1}{2} + \frac{1}{3} + \dots + \frac{1}{n} \approx 5.18.$$
 (2)

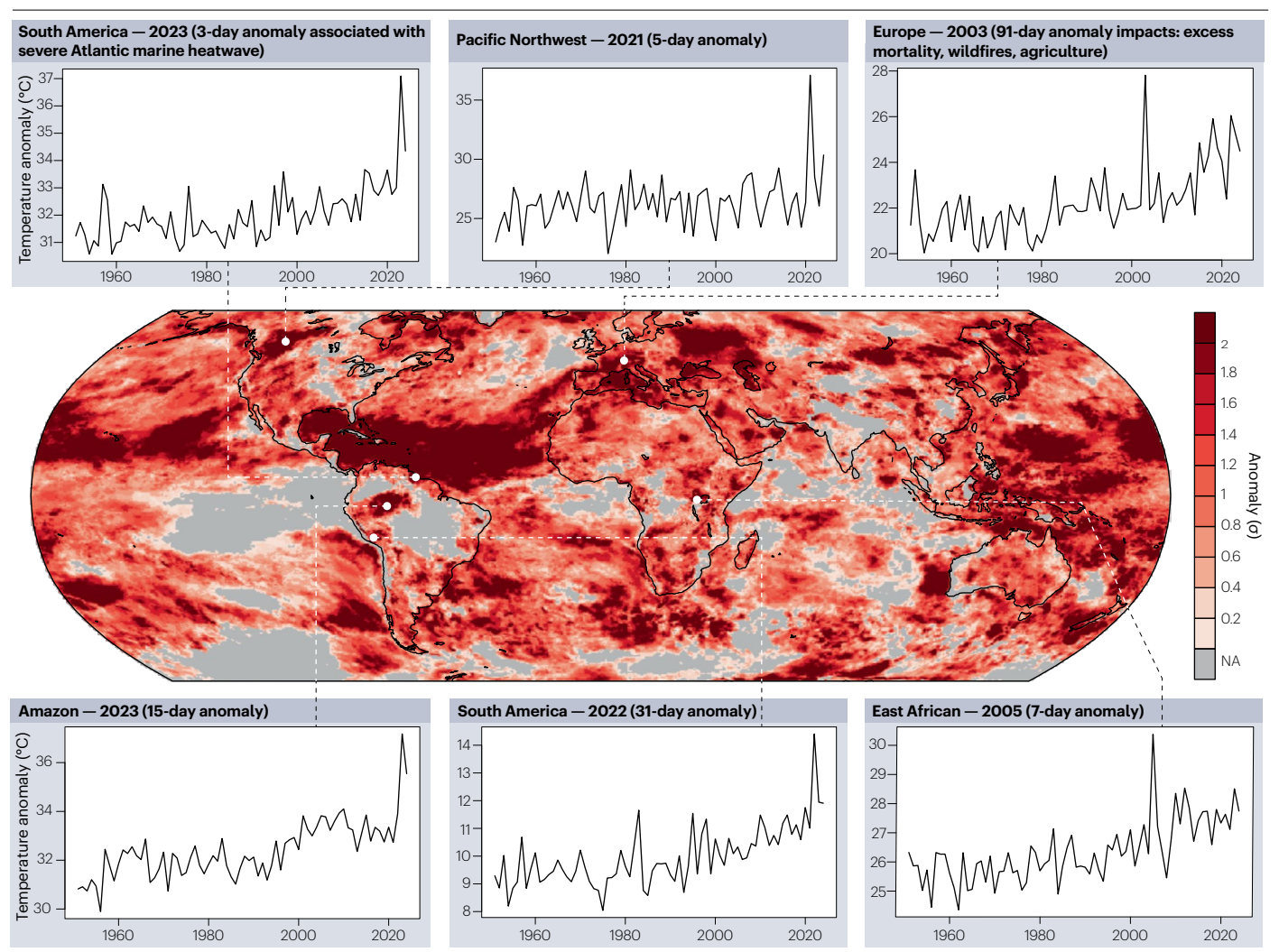
However, the number of expected events does not increase substantially with record length 35,38,39 , reaching 7.48 when n = 1,000 and 9.79 when n = 10,000. These results express the rarity for records to be broken in the i.i.d. setting if n is sufficiently large.

The reality of climate change challenges these simplistic assumptions. Records for certain climate variables, such as hot extremes, occur much more frequently (and cold extremes less frequently) than expected under a stationary climate $^{33,40-42}$. Indeed, under a Gaussian distribution with a linear trend (ν) in the mean and a constant standard deviation (σ), records are broken at an approximate rate of 1/n + K(n), in which K(n) varies with n very slowly and is proportional to the ratio of the trend to the standard deviation 42 . For large n and small ν/σ ,

$$Pr(record) = Pr\{X_n > \max(X_1, ..., X_{n-1})\} \approx \frac{1}{n} + \frac{\nu}{\sigma} \frac{2\sqrt{\pi}}{e^2} \sqrt{\log\left(\frac{n^2}{8\pi}\right)}. \quad (3)$$

Hence, with a long-term increasing linear trend, the record probability will be larger than expected in the simplistic i.i.d. setting.

Assessment of statistical records is not limited to these basic scenarios. Record-breaking and record-shattering extremes under more complex forms of non-stationary forced scenarios have also been investigated^{28,43}, as has the precise probabilistic behaviour of record occurrences for stationary but temporally correlated Gaussian sequences⁴⁴. Record statistics have also been exploited to provide evidence for a warming climate⁴², and in the context of detection and attribution under both 'factual' and 'counterfactual' scenarios⁴⁵⁻⁴⁷, given that any deviation from the 1/n trend is a potential sign of climate change if data are independent.



 $\label{eq:Fig.1} \textbf{Fig.1} | \textbf{Example record-shattering hot extremes.} \text{ The largest record hot margins (that is, the difference from the previous record, expressed as standard deviations) in ERA5 (ref. 160) since the year 2000. Annual maxima of 1-day, 3-day, 5-day, 7-day, 11-day, 21-day, 31-day, 61-day and 91-day running mean temperatures are standardized with the respective standard deviation over 1950–1980. Regions where the record has not been broken since 2000 are in grey. For regions$

where the record was broken at different timescales, the biggest record margin across all timescales and years is plotted. Inlet panels illustrate the six largest standardized record margins over land across all timescales over 2000–2024. A large fraction of the globe has experienced record-shattering hot extremes within the period 2000–2024. NA, not available.

The size of record margins is also an important consideration. Intuitively, record margins (expressed in absolute units or standard deviations) could be expected to decrease under stationarity. However, that is not generally the case. Consider data following the generalized Pareto distribution (GPD) with scale $\tilde{t} > 0$ and shape $\tilde{\xi}$ parameters, which is motivated by extreme-value theory for modelling high threshold exceedances³⁷. Under the i.i.d. assumption (thus, stationarity), the distribution of record margins will be constant in time for a light-tailed GPD (namely, the exponential distribution arising when $\tilde{\xi} = 0$). By contrast, record margins will tend to increase with time for a heavy-tailed GPD with $\tilde{\xi} > 0$, whereas they will tend to decrease with time for a bounded-tailed GPD with $\tilde{\xi} < 0$ (Supplementary information and Supplementary Fig. 3). Therefore, the behaviour of record margins must be interpreted with care when used to infer the strength of the climate change signal.

Record-shattering extremes

Beyond record breaking, a record-shattering extreme event is one whose magnitude exceeds all previous observations by a fixed positive margin of at least c > 0. If the random variables $\{X_i; t=1,...,n\}$ are mutually independent with continuous cumulative distribution function, F_t , and with probability density function, f_t , then the probability of a record-shattering event²⁸ is:

$$Pr(\text{record-shattering event}) = Pr\{X_n > \max(X_1, ..., X_{n-1}) + c\}$$

$$= E_{X_n} \{Pr(X_1 < X_n - c, ..., X_{n-1} < X_n - c | X_n)\}$$

$$= \int \{ \prod_{i=1}^{n-1} F_t(x - c) \} f_n(x) \, dx.$$
(4)

When c = 0, equation (4) corresponds to the standard probability of record breaking. The choice of the constant c used to define

record-shattering extremes is somewhat arbitrary and application-wspecific. As a general rule, it should be large enough to differentiate record-shattering from record-breaking events, such as one standard deviation when the distribution F_t is Gaussian-like or relatively light-tailed — other choices might be more suitable for strongly skewed and heavy-tailed distributions.

Although no analytical solution of the integral in equation (4) is available in general, standard numerical techniques can be used to accurately approximate the corresponding probabilities. Hence, equation (4) can be used to compute probabilities for various record-shattering thresholds \boldsymbol{c} and under changes in various distributional parameters over time (location parameter or higher moments). However, such parameters, which must be specified, might be imperfectly known in practice.

In certain cases, extremes might be driven by different physical mechanisms. The assumed marginal distribution, F_{t} , thus becomes a mixture of distributions rather than an individual distribution. Nevertheless, equation (4) remains valid. For example, with frontal and convective precipitation, the distribution F_t might be a mixture between two distributions with different tail heaviness. For illustration, assume that one of these mixture components (for example, convective precipitation) has a heavy tail, whereas the other (frontal precipitation) has a light tail; then, in this case and under a stationary climate, the mixture component that has the heaviest tail will eventually dominate the occurrence probability of record-breaking or record-shattering events, and record statistics will thus only be affected (in the limit) by a single underlying mixture component (and its mixture probability). Perhaps, the biggest difference in this case is that if $p \in (0, 1)$ denotes the mixture probability of the heaviest-tailed mixture component and *n* the total sample size, there will be, on average, only roughly np < nobservations contributing to record events rather than *n* had they all been drawn from the heaviest mixture component, slowing down the record-breaking rate.

Illustration of record-shattering calculations

Record-shattering probabilities can be computed from equation (4) for various data sets. Here, its functionality is illustrated using a record of changes in the annual hottest 5-day period (Tx5d) averaged across the Pacific Northwest in the 100-member Community Earth System Model version 2 large ensemble (CESM2-LE) forced with SSP3-7.0 (Fig. 2; 'scenario 4', Supplementary Fig. 4), similar to ref. 28; the mean trend and standard deviation is smoothed using a spline-based additive model. The impact of the warming trend on record-shattering probabilities is also illustrated using three idealized temperature scenarios²⁸: no warming (Fig. 2; 'scenario 1'); no warming followed by linear warming (Fig. 2; 'scenario 2'); and no warming followed by linear warming and stabilization (Fig. 2; 'scenario 3'). All four scenarios follow either the Gaussian or the generalized extreme-value (GEV) distribution in an independent but non-stationary setting. These distributions are widely used and appear as limiting models for averages and maxima, respectively; they thus cover a wide range of situations and the results can be expected to be relatively robust to the assumed distribution, at least qualitatively. To each of these scenarios, the impact of the forced response on the annual probability of a record-shattering event is assessed (Fig. 2). For these examples, results are presented for 1σ -records, with c = 1.67 in equation (4).

The temporal evolution of warming in each scenario has a direct distinct impact on record-shattering probabilities (Fig. 2c). Figure 2c displays the corresponding record-shattering probabilities when assuming that F_t is the Gaussian distribution with mean μ_t driven by the trends displayed in Fig. 2a and a changing standard deviation

 σ_t shown in Fig. 2b as estimated from the CESM2-LE⁴⁸ or set to the displayed idealized scenarios.

Fast mean temperature increases lead to increasing record-shattering probabilities. The record-shattering probability is thus dependent on the forced warming rate or speed of warming. This effect is seen in the CESM2 simulations (onset of fast warming around 1975) and scenarios 2 and 3 with a fast warming onset in 2000 (Fig. 2c, red and orange lines). Trends that flatten instead lead to a quick decline, as apparent in the no-warming scenario 1 after 1850, and for scenario 3 after temperature stabilization in 2050 (Fig. 2c). In addition to the effect of the warming rate, increases in the standard deviation lead to increases in record-shattering probabilities. This effect is seen for the CESM2 simulations: there is a noticeable difference when the standard deviation is treated as non-stationary, and the more flexible fully non-stationary Gaussian model captures large record probabilities more accurately in this case (Fig. 2c, solid and dotted lines). Similar conclusions can be drawn based on scenarios 2 and 3.

Extreme-value theory motivates the use of the GEV distribution for modelling extreme events defined as annual maxima³⁷, so it is a natural distribution to consider to assess the impact of the tail heaviness on record-shattering behaviour. The distribution F_t is thus now specified as the GEV distribution with location $\tilde{\mu}_t$, scale $\tilde{\sigma}_t > 0$ and shape $\tilde{\xi}$ parameters. A GEV model is fitted using a generalized linear model in which $\tilde{\mu}_t = \beta_0 + \beta_1 x_t^{\mu}$ with covariate x_t^{μ} being the smoothed CESM2-LE mean and where \tilde{o}_t is treated either as constant or modelled as $\tilde{\sigma}_t = \gamma_0 + \gamma_t x_t^{\sigma}$ with covariate x_t^{σ} being the smoothed CESM2-LE standard deviation. The shape parameter $\tilde{\xi}$ is kept constant over time. The corresponding estimated 1*o*-record probabilities fit the empirical record curve even slightly better than the Gaussian distribution (Fig. 2d). To assess the effect of the GEV shape parameter in more detail, it is now fixed to $\xi = -0.3, ..., 0.3$ (from bounded upper tails to heavy tails), and the GEV model is refitted in both $\tilde{\mu}_t$ and $\tilde{\sigma}_t$. The resulting record-shattering probabilities (Fig. 2e) illustrate that tail behaviour has an impact on record probabilities: bounded tails (with $\tilde{\xi} < 0$) initially exhibit fast reductions in record-shattering probabilities, whereas heavy tails (with $\tilde{\xi} > 0$) instead decline more slowly. Interestingly, the warming trend impacts record-shattering probabilities more under bounded tails than under heavy tails (for which the behaviour is more 'stable' with time). With the increasing location and scale parameters over time, GEV distributions with intermediate shape parameters (zero or slightly negative) show the highest record-shattering probabilities around the end of the century.

Compound records

In some events, records are broken simultaneously in multiple impact-relevant variables⁴⁹. For instance, a record heat and dry event was observed during the 2018 growing season in Germany. Thus, it is important to consider compound record-shattering probabilities for bivariate extreme events, which can be computed as:

Pr(compound record-shattering event)
$$= \Pr\{X_n > \max(X_1, ..., X_{n-1}) + c_x \text{ and } Y_n > \max(Y_1, ..., Y_{n-1}) + c_y\}$$

$$= \iint \left\{ \prod_{t=1}^{n-1} F_t(x - c_{x'}, y - c_y) \right\} f_n(x, y) \, dx \, dy,$$
(5)

in which $\{(X_t, Y_t)^T; t=1, ..., n\}$ is now a sequence of independent bivariate random vectors with joint cumulative distribution function F_t and joint probability density function f_t , for some constants $c_x > 0$, $c_y > 0$. To examine how the dependence between X_t and Y_t affects the

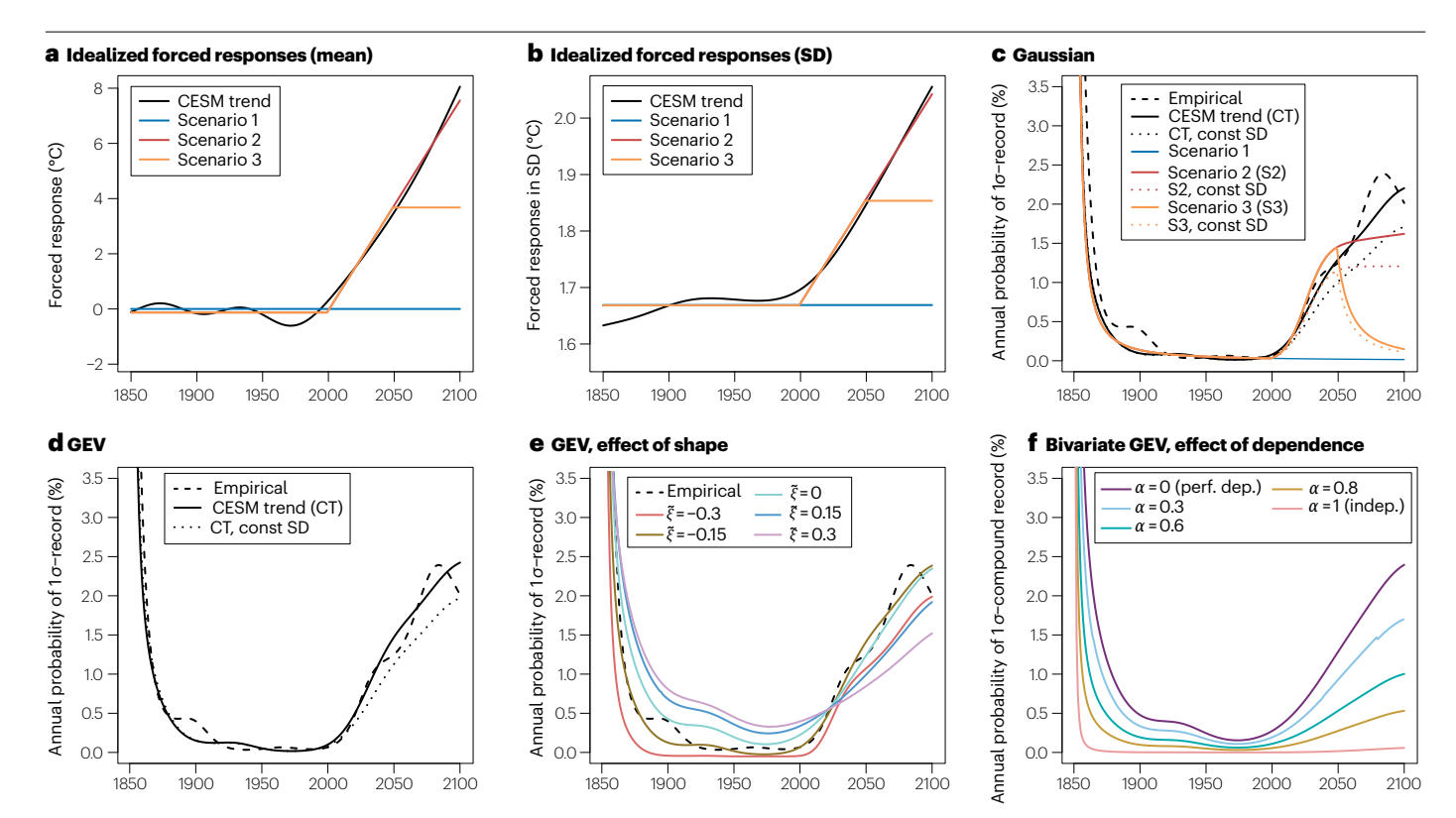


Fig. 2| **Statistical characteristics of record extremes. a**, Mean trend of the hottest 5-day period per year in the Pacific Northwest region as simulated by climate model and prescribed in idealized statistical scenarios. Smoothed CESM2-LE mean trend as an estimate of the forced response that is the change to external forcings in the absence of internal variability (CESM trend; black; same domain as ref. 143), and selected idealized scenarios with no warming (scenario 1; blue), no warming followed by linear warming (scenario 2; red) and no warming followed by linear warming and stabilization (scenario 3; orange). **b**, As in panel **a**, but the forced trend in the standard deviation (SD). **c**, Annual probability of 1*o*-records computed empirically (black dashed), and for each scenario displayed in panels **a** and **b**, assuming a Gaussian distribution with changing SD (solid) or constant SD (const SD; dotted). **d**, 1*o*-record probabilities based on a generalized extreme-value (GEV) distribution using the

non-stationary CESM2-LE mean trend as a covariate to the location parameter (solid black), non-stationary mean and variance (dotted black) and computed empirically as in panel \mathbf{c} (black dashed). \mathbf{e} , As in panel \mathbf{d} but illustrating the sensitivity of 1σ -records to different GEV shape parameters $\vec{\xi}=-0.3,...,0.3$ (red to purple lines) and estimating smooth location and scale parameters using generalized additive models (GAMs). \mathbf{f} , Compound record-shattering probabilities, assuming a bivariate GEV distribution in which margins are both Gumbel distributions with non-stationary location and scale parameters (driven by CESM2-LE smooth trends) and with logistic extreme-value dependence structure with parameter $\alpha \to 0$, $\alpha = 0.3, 0.6, 0.8, 1$ (purple to red curves from perfect dependence to independence, respectively). The record probability is highly dependent on the warming trend and the characteristics of the statistical distribution of a variable.

probability of compound record events, both margins are set to the fitted GEV distribution with non-stationary $\tilde{\mu}_t$ and $\tilde{\sigma}_t$ and constant $\tilde{\xi}=0$ (Fig. 2), choosing the same non-stationary light-tailed marginal behaviour for X_t and Y_t . The dependence structure between X_t and Y_t is further specified as the logistic extreme-value model so, parametrized by a single dependence parameter $\alpha \in (0,1]$ (assumed to be time constant) interpolating between perfect dependence $(\alpha \to 0)$ and independence $(\alpha = 1)$.

The resulting record-shattering probabilities (Fig. 2f) reveal that the strength of dependence between X_t and Y_t largely determines the occurrence probability of joint records. This relationship arises because a higher dependence leads to more compound exceedances⁴⁹, which should therefore be accounted for when assessing risks of compound extreme record events.

Hot and cold records

Record-breaking hot and cold events often lead to serious socioeconomic and ecological impacts. Their occurrence is dependent on the event duration (daily up to annual timescales); whether they are all-time records (Fig. 3a) or records for a particular day, month (Supplementary Fig. 5) or season; and the length of the observational record (equation (2)). Changes in the frequency of temperature records can be quantified using the record ratio: the ratio of the observed frequency of record events to the one theoretically expected in a stationary climate (Fig. 3a). Using the record ratio, observed and projected changes in record-breaking heat and cold are now discussed.

Observed changes at global scale

The occurrence of hot and cold records has evolved markedly over the observational era and, since the 1980s, deviates strongly from expectations in a stationary climate $^{24-26,51}$. Over land, observations and reanalysis indicate that the all-time heat record ratio during 2016–2024 was -4.1 (Fig. 3a; red). That is, the global occurrence of daily hot records was more than four times higher than expected without climate change; values are similar for ERA5 and BEST observations. The highest record ratio over land was in 2023 and 2024, reaching 5.5 and 6.2, respectively.

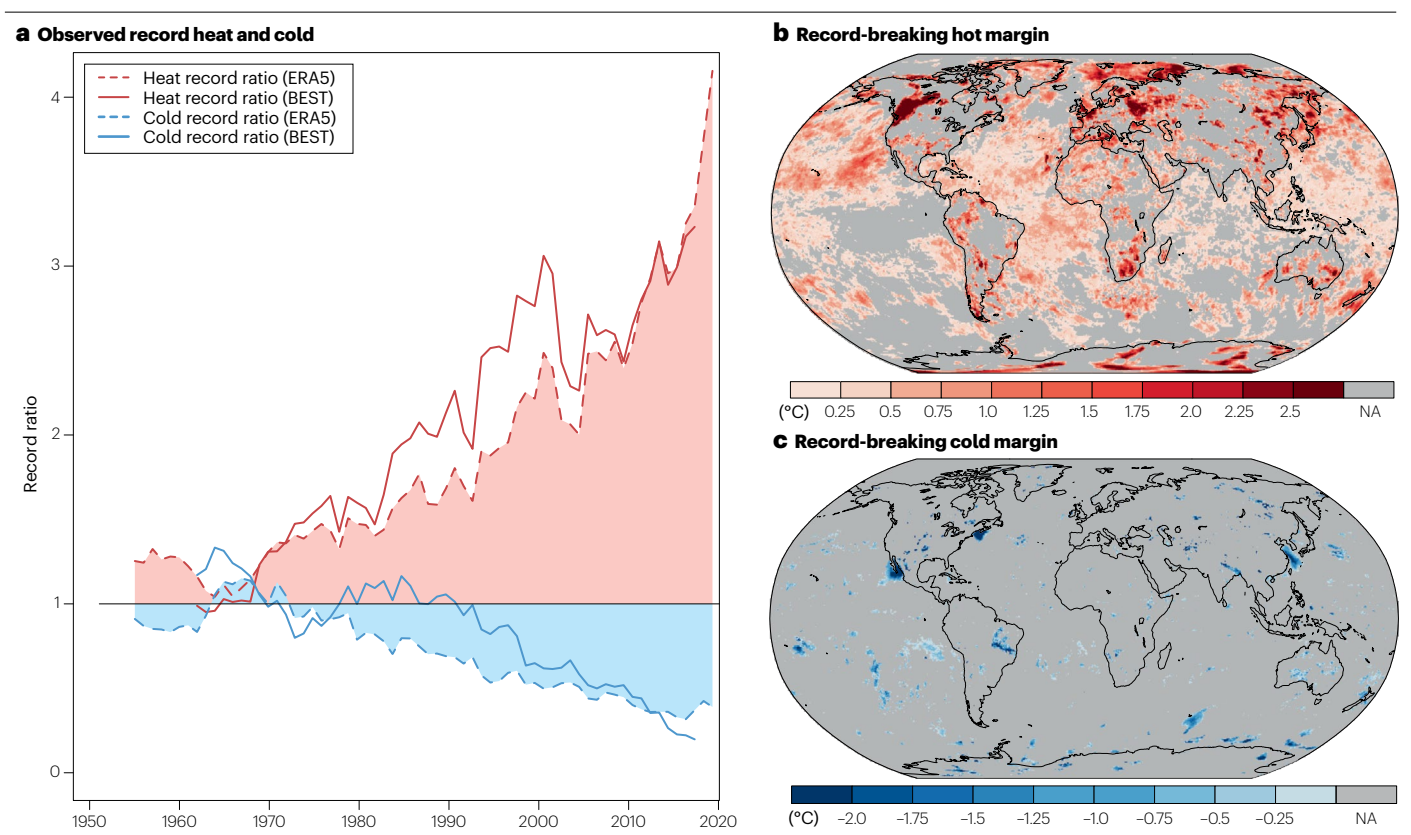


Fig. 3 | **Observed change in record hot and cold. a**, The observed heat (red) and cold (blue) record ratio in ERA5 (ref. 160) (dashed) and BEST⁵² (solid). The record ratio is calculated as the probability of all-time daily record hot or cold temperatures across global land regions relative to the theoretically expected occurrence in a stationary climate. Record frequencies are calculated at the grid-point level, averaged across global land regions and then smoothed with a

9-year running mean. **b**, The maximum record-breaking hot margin (that is, the difference from the previous record) over 2010–2024 from ERA5; grey values indicate that no all-time record heat was observed. **c**, As in panel **b**, but the all-time cold record margin. A large fraction of the globe has experienced all-time hot records, whereas a very small fraction has experienced cold records in the period 2010–2024. NA, not available.

By contrast, the cold record ratio was ~0.5 in ERA5 and ~0.2 in BEST during 2016–2024 and 2014–2022, respectively, suggesting that cold record occurrence was 20–50% of that theoretically expected without climate change (Fig. 3a; blue). Record ratios for daily records per month rather than per year are broadly consistent (Supplementary Fig. 5). Looking spatially, 62% and 8% of the land surface witnessed recording-breaking daily hot and record-breaking cold since 2010, respectively (Fig. 3b,c), further reinforcing the rarity of new cold records over land.

These findings are consistent with other literatures. For instance, the observed record ratio (BEST gridded data set⁵²) for monthly mean hot temperatures was -5 in 2001–2010 (ref. 53) and reached -8 in 2011–2020 (ref. 54). For monthly temperature, the record ratio is closely related to the ratio of warming trend to short-term standard deviation^{43,55,56}, consistent with the fact that the record probability is proportional to the ratio v/σ (equation (3)). Therefore, the record ratio is substantially larger and a climate change signal can be detected earlier over the tropics where day-to-day and year-to-year variability (σ) is lower than in the high latitudes^{54,57}. Likewise, the record ratio is higher for longer aggregation timescales such as monthly (Supplementary Fig. 7), seasonal or annual means, for which the variability is lower but the signal is broadly the same^{58,59}.

These record hot and cold signals are equally or even more pronounced over the oceans. Indeed, record-breaking heatwaves have been observed in sea surface temperature across ocean basins 60,61, where marine heatwave days have doubled between 1982 and 2016 (ref. 62). Hot records are more frequent in air temperature over the ocean (record ratio ~5.5 in 2016-2024) and cold records less frequent (record ratio ~0.3 in 2016-2024) than expected without warming (Supplementary Fig. 6). These record ratios are as high or even higher than over land owing to the proportionality of the trend to variability v/σ , which tends to be higher as a result of lower variability. In addition to the higher magnitude, the spatial area exhibiting record temperatures is also higher than land areas (Fig. 3b,c). Indeed, the frequency hot records were higher than expected without warming in more than 87% of the world's oceans²⁷. The occurrence of these sea surface temperature records in any given year is strongly affected by El Niño/Southern Oscillation, as demonstrated by various records being broken during the 1997/1998 El Niño. In the ocean, there are also regions where record statistics distinctly deviate from expectations of a homogeneous warming trend such as parts of North Atlantic warming hole, where the record behaviour is consistent with the expected lack of warming or even slight local cooling trend²⁷.

Balance of hot events to cold events

Clear signals in record-breaking hot occurrence have also been identified at regional scales. These signals are particularly prominent in the ratio of hot-to-cold records (hereafter, hot-to-cold record ratio), defined as the frequency of hot divided by the frequency of cold records; in a stationary climate, the hot-to-cold record ratio is expected to be -1.

The hot-to-cold record ratio varies substantially by region. In Europe, the USA and China, the hot-to-cold record ratio has deviated from 1 (refs. 24-26,63), evolving at rates influenced by contrasting warming trends and internal variability (proportionality with v/σ). For instance, in the USA (where there are relatively weak trends in annual temperature maxima^{64,65}), the hot-to-cold record ratio reached 2 in the early 2000s^{24,66,67}. In Australia, the ratio was about 12 over 2000–2014 (which cannot be explained by modes of variability in the Pacific⁶⁸), and in China it was ~3 over 1995-2004 (ref. 63). In Europe, the hot-tocold record ratio reached ~4 in 2010 (refs. 25,26,55) and continued to increase thereafter; the higher changes linked to pronounced trends in annual temperature maxima owing to anticyclonic conditions $^{65,69-71}$ and declining aerosol concentrations⁷². Nevertheless, the observed European hot-to-cold record ratio is still within the range of internal variability, with projections that anthropogenic signals will emerge for the summer season in the 2020s⁵¹. Although decadal variations in ratios could regionally relate to internal decadal variability, aerosol-induced cooling delayed the detectability of a substantial human contribution to record-breaking hot extremes⁷³. Methodological differences also contribute to contrasts in regional hot-to-cold record ratios.

Increases in the frequency of hot records are not the only factor contributing to this rising hot-to-cold record ratio. Record cold events have been declining faster than would be expected in stationary climate — globally (Fig. 3b) and across many regions such as Europe 25,51,59,74 , the USA 24,67 , Australia 68,75 and China 63 — contributing to this change. There is no observational evidence for more record cold events resulting from cold air outbreaks or changes in atmospheric circulation 76 . On the contrary, in many places, changes in coldest days and nights are even more pronounced than the mean warming 77 owing to a regional reduction of winter temperature variability 26,78,79 . Thus, thermodynamic changes are the dominant factor leading to less cold records, consistent with the observed reduction of very cold nights and days and the pronounced warming of the cold nights and days 80 .

Record statistics can be used for detection and attribution to anthropogenic warming $^{45-47}$. The detectability tends to be higher for hot-to-cold ratios than for the record ratio of cold and hot records individually because there is a climate change signal in both. Hot and cold extremes (and thus records) are controlled by different mechanisms, but both are affected by warming mean temperatures. Quantifying the ratio of their occurrence is a way of optimizing the detectability of a warming signal. The strongest signal has been identified in global mean temperature record events (Supplementary Fig. 1) owing to the large ratio of trend ν to variability $\sigma^{81,82}$ (Fig. 3b).

Projected changes in temperature records

These observed trends towards more record hot and fewer record cold events will continue and intensify in the near future ^{24,51,53}. For instance, by the end of the twenty-first century, record ratios for daily all-time hot records over global land are projected to reach: -19.7 for SSP5-8.5; -15.7 for SSP3-7.0; -7.3 for SSP2-4.5; -2.9 for SSP1-2.6 and -1.8 for SSP1-1.9 (Fig. 4a). Under all emission scenarios, the heat record ratio continues to increase until the 2030s, before declining in the low (SSP1-2.6) and

very low (SSP1-1.9) emission scenarios, stabilizing in the intermediate emission scenario (SSP2-4.5) and increasing at pace in the high (SSP3-7.0) and very high (SSP5-8.5) emission scenarios. In the low and very low emission scenarios, record probability declines because the record occurrence depends on the rate of warming. Thus, a slowing mean temperature trend would lead to a slight reduction in the record ratio of hot extremes, and a stabilization of mean temperatures would lead to a rapid reduction, highlighting the benefits of mitigation.

There is robust evidence from numerous studies for projected increases in the occurrence of heat records with ongoing warming. For instance, under an intermediate emission scenario, the global average record ratio for monthly hot records is projected to exceed 12 by the $2040s^{53}$. Moreover, the annual hot record of the twentieth century could be broken more than 99% of the Earth's surface by 2080 (ref. 57). More regionally in Europe, summer daily warm records are $10\times$ more likely by the end of the twenty-first century than before the 1980s in CMIP5 models forced with RCP8.5, consistently projecting amplified increases in hot record occurrences over the Mediterranean basin 51 . Any regional and seasonal differences largely relate to the signal-to-noise ratio of the changes 25,26 .

The occurrence of record-shattering hot extremes is also projected to increase 1,28,83 . For instance, in a very high emission scenario (RCP8.5), week-long hot extremes that break records by three or more standard deviations are 2–7 and 3–21 times more probable in 2021–2050 and 2051–2080 compared with 1981–2010, respectively 28 . Likewise, the probability of at least one monthly record breaking the previous record by more than 1 °C is 8.9 in a very high emission scenario and 1.1 in a low emission scenario 83 . Given the high ratio of trend ν to variability σ , the probability of daily to weekly record-shattering hot extremes is projected to be largest in the northern mid-latitudes 28 and of monthly record-shattering extremes in the tropics 83 . The increase in record-shattering extremes is consistent with theoretical statistical considerations.

Although the frequency of record-breaking and record-shattering heat continues in the future, the frequency of cold records diminishes further. Cold records decline in all emission scenarios, with record ratios for global land reaching -0.07 and 0.09 for SSP1-1.9 and SSP1-2.6, and less than -0.05 for the other scenarios by 2050 onwards (Fig. 4b); thus, the likelihood of new cold records over land becomes negligible. These changes are also evident regionally, including in Europe where breaking a new daily cold record is projected to be extremely difficult in the last three decades of the twenty-first century⁵¹ and in the USA where the hot-to-cold record ratio is projected to reach 20 and 50 by the mid and late twenty-first century, respectively²⁴.

Hydrological records

Along with temperatures, record-breaking events are also observed in the water cycle. Indeed, precipitation variability is expected to increase across various timescales states, reflecting observed increases in the intensity and frequency of heavy precipitation extremes. Such events include the extreme downpours during the Copenhagen cloudburst 2011 (ref. 85), the Boscastle floods states, the Henan floods states, the 2021 European rainfall record of Rossiglione the daily to multiday events such as the UK wettest day on record in October 2020 (ref. 88) and the 2021 rainfall events in northwestern Germany, Belgium and the Netherlands states, and the multiday events such as the 2005 flooding in the Alps states, and the most record-shattering precipitation extremes are illustrated in Supplementary Fig. 2. In addition to amplifying heavy precipitation extremes, climate change has contributed to increases in agricultural

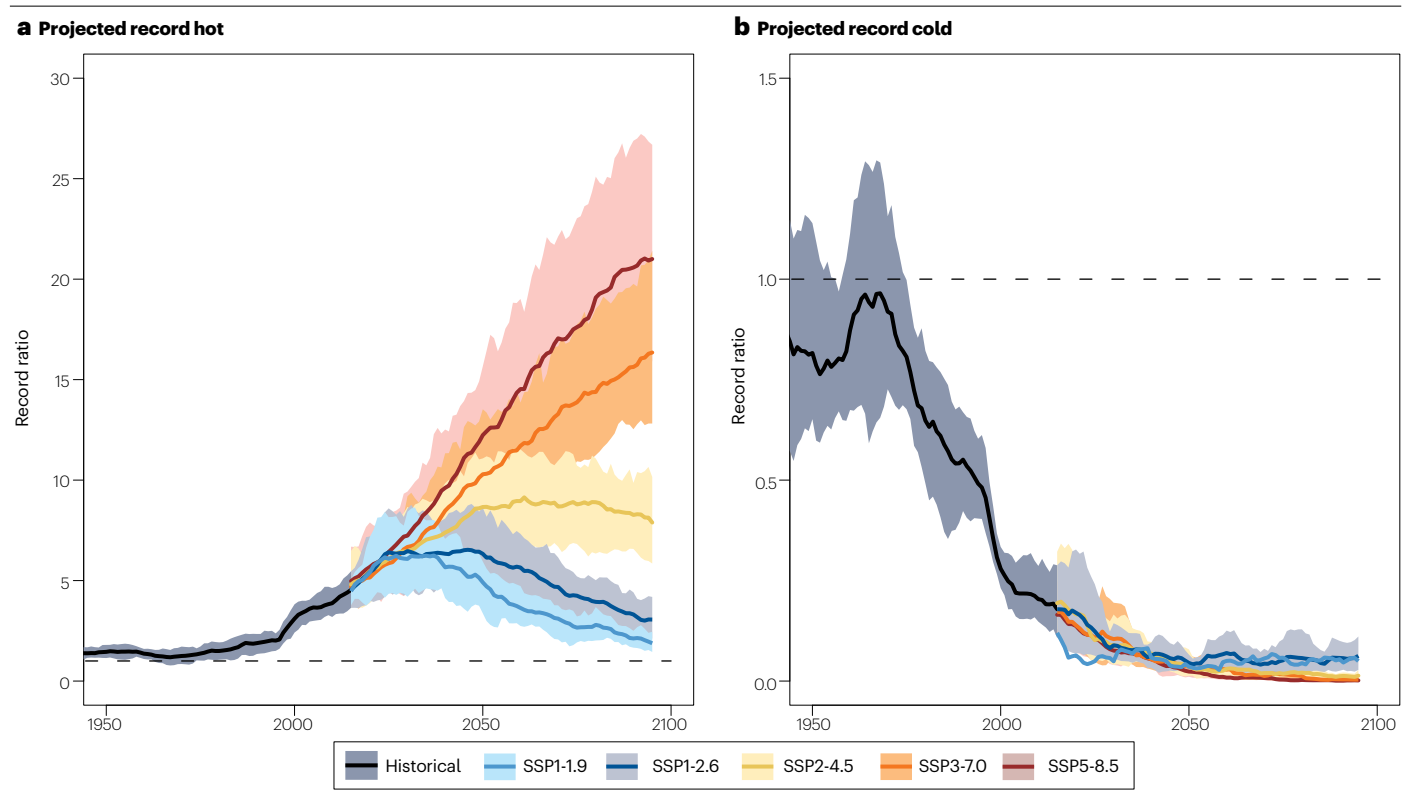


Fig. 4 | **Projected changes in record hot and cold. a**, Modelled heat record ratio in CMIP6 simulations forced with historical (grey), SSP1-1.9 (light blue), SSP1-2.6 (dark blue), SSP2-4.5 (yellow), SSP3-7.0 (orange) and SSP5-8.5 (dark red) scenarios. The record ratio is calculated as the probability of all-time record daily hot or cold temperatures across global land regions relative to the theoretically expected occurrence in a stationary climate. Probability ratios are calculated at

the grid-point level and area-weighted across the globe. Thick lines represent the multimodel mean and shading the 5-95% range. \mathbf{b} , As in panel \mathbf{a} but for record cold events. Scenarios with rapid and high warming yield very high hot record ratios, whereas scenarios with slowed warming or stabilized mean temperatures yield declining hot record ratios.

and ecological droughts in some regions owing to increased land evapotranspiration, and in some cases, a reduction in seasonal precipitation. Observed and projected changes in record-breaking wetness (heavy rainfall) and dryness (drought) are now discussed. Note, gridded reanalysis and observational precipitation data include substantial uncertainties and, as such, their respective record statistics need to be interpreted with caution.

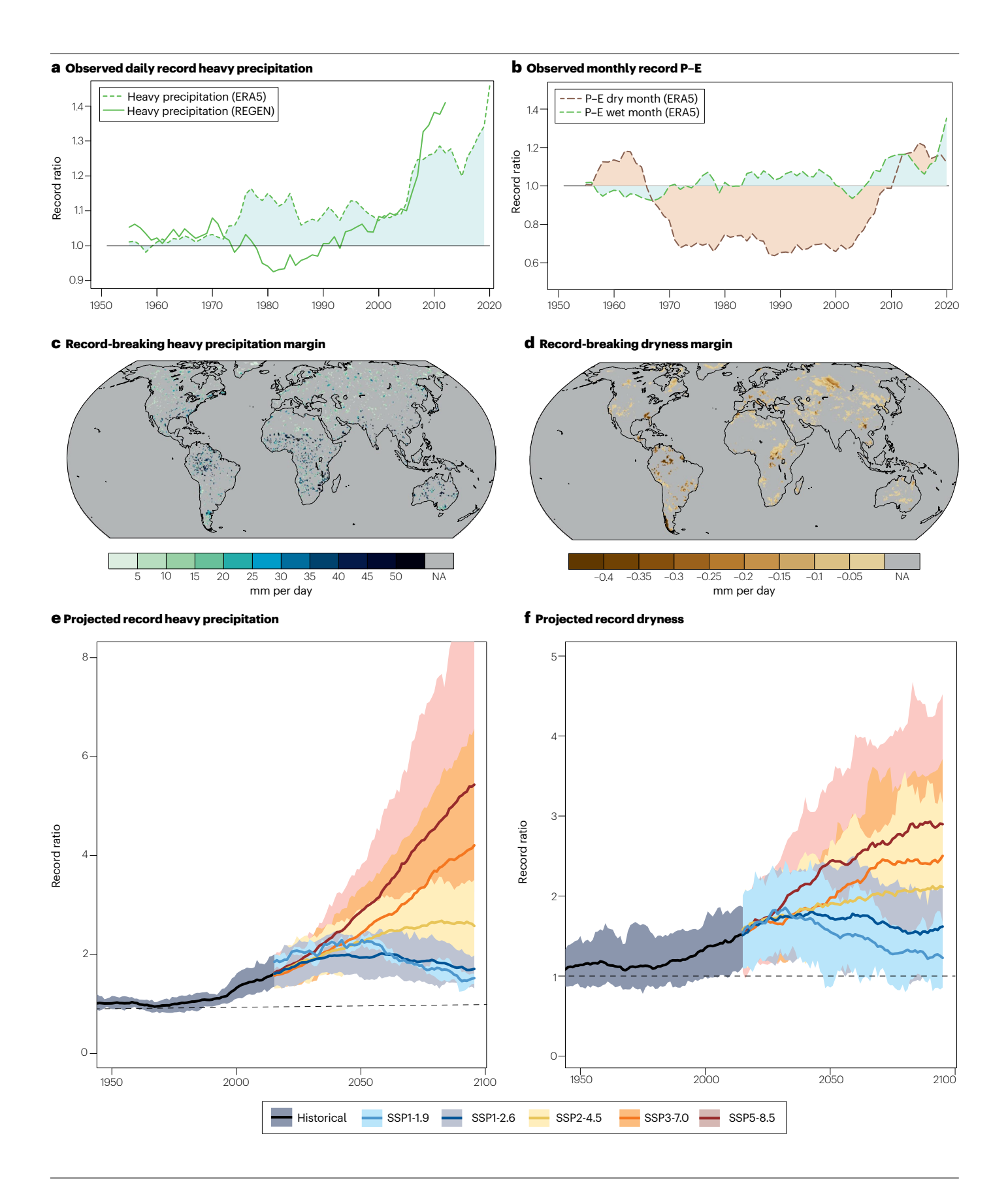
Observed record-breaking heavy precipitation and dryness

Similar to hot temperatures, there has been a general tendency towards increasing frequency of record-breaking heavy precipitation. Although there is substantial observational uncertainty and large

internal variability 90 , this tendency is broadly consistent across data sets (Fig. 5a). Over land, the annual 1-day maximum precipitation record ratio during 2016–2024 was ~1.45 for ERA5 and ~1.41 during 2015–2023 for the REGEN gridded observational data set 91 , meaning the number of precipitation records observed today is more than 40% higher than expected in a stationary climate. These increases in precipitation records have become more pronounced since the year 2000. Many of the record-breaking precipitation events were also record-shattering extremes, with distinct large record margins. This change is also due to the typically heavy-tailed distribution of hourly and daily precipitation, which leads to an increase in record margins over time even in a stationary climate and even more so in a warming climate. Spatially,

Fig. 5 | **Observed and projected change in record heavy precipitation and dryness over land. a**, Observed record precipitation ratios in ERA5 (ref. 160) (dashed) and REGEN⁹¹. The record ratio is calculated as the probability of all-time record 1-day precipitation across global land regions relative to the theoretically expected occurrence in a stationary climate. Record frequencies are calculated at the grid-point level, averaged across global land regions and smoothed with a 9-year running mean. **b**, As in panel **a**, but for record monthly maximum (green) and minimum (brown) precipitation-minus-evaporation (P–E) in ERA5. **c**, The maximum record-breaking 1-day heavy precipitation margin (that is, the difference from the previous record) over 2010–2024 from ERA5; grey values

indicate regions where the annual 1-day maximum precipitation record was not broken. **d**, As in panel **c**, but for monthly dry anomalies (a negative P–E record). **e**, Modelled record precipitation ratios for all-time record 1-day precipitation across global land regions as simulated in CMIP6 models forced with historical (grey), SSP1-1.9 (light blue), SSP1-2.6 (dark blue), SSP2-4.5 (yellow), SSP3-7.0 (orange) and SSP5-8.5 (dark red) scenarios. Thick lines represent the multimodel mean and shading the 5–95% range. **f**, As in panel **e**, but for record monthly dryness (P–E). Observed and projected record ratios in heavy precipitation and dryness show a signal of climate change. NA, not available.



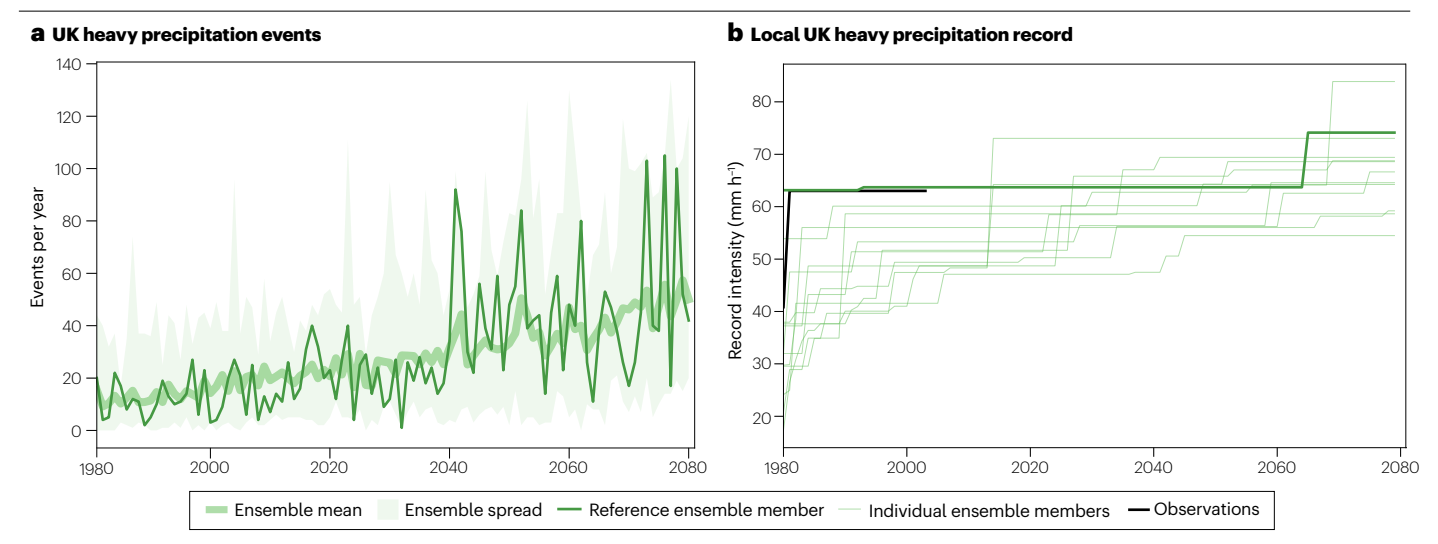


Fig. 6 | Evolution of hourly precipitation in the UK. a, Number of events per year exceeding 20 mm h $^{-1}$ at the 12 km scale from 1981 to 2080 in a convection-permitting model. The thinner line represents the reference member, the thick line the ensemble mean of 12 members and shading the ensemble min–max range. Threshold exceedances occurring within a UK subregion on the same day are considered part of a single event. **b**, The highest annual maximum hourly

precipitation recorded at any 12 km grid point across the UK since the start of the simulations in 1980. The bold line represents the reference ensemble member and the thin lines the individual ensemble members. The regional occurrence of record precipitation is strongly affected by internal variability. Panel ${\bf b}$ adapted with permission from ref. 103.

changes are observed across many land regions (Fig. 5c), but individual records are typically broken over relatively small locations given the scale at which precipitation extremes occur. Other analyses support increases in 1-day heavy precipitation, including based on HadEX2 observations in which the record ratio over 1981–2010 was ~1.2 (ref. 31). These changes are in keeping with thermodynamic considerations based on the Clausius–Clapeyron relationships.

Observed increases in heavy rainfall records are not limited to 1-day totals. Indeed, the smoothed record ratio for global-mean record-wet months is almost 1.2 in 2013, indicating that these extremes are 20% higher than expected in a stationary climate³². This signal primarily comes from pronounced changes in the northern mid-to-high latitudes where the occurrence of record-wet months has increased by up to 37% in Northern Europe³². Precipitation—evaporation (P–E) wet months also reveal record ratios of 1.35 from 2016 to 2024, providing further supporting evidence for increasing record-breaking wet months (Fig. 5b).

At the other end of the hydrological spectrum, changes in the frequency of record droughts have also been observed. Several contemporary droughts have been described as record breaking at least in the observational period⁴⁹ and, in some cases, even across parts of the paleoclimate record^{92,93}. Assessing monthly P–E dry months in ERAS, for example, reveals large decadal to multidecadal variations (Fig. 5b). Yet, there seems to be a weak tendency towards a higher occurrence of monthly dry records since -2013 than expected in a stationary climate (Fig. 5b), such that the record ratio over 2016–2024 is 1.12. These record dry months are scattered across all global land regions with no clear spatial pattern (Fig. 5d). Given the different types of droughts (meteorological, hydrological, agricultural and ecological), their contrasting timescales (short flash droughts to decadal ecological droughts), complex spatial scales and potential low-frequency variability, assessing their record-breaking character is challenging⁹⁴ and

can lead to conflicting statements ^{92,95}. Indeed, other record statistics show variations even in the sign of the drought record ratio, perhaps relating to the complex interactions between anthropogenic aerosol forcing and greenhouse forcing ^{96,97} in combination with unforced internal variability. As such, it remains unclear to what extent changes in drought record statistics are a climate change signal.

$\label{projected} \textbf{Projected changes in record-breaking extremes in the water cycle}$

Along with warming temperatures, the intensity and frequency of precipitation extremes are projected to increase across most global land regions. The annual 1-day maximum precipitation record ratio for global land regions is ~2 for all scenarios by 2050 (Fig. 5e). Record ratios diverge thereafter, and by the end of the twenty-first century, multimodel mean values reach ~5.6 for SSP5-8.5, ~4.3 for SSP3-7.0, ~2.7 for SSP2-4.5, ~1.8 for SSP1-2.6 and ~1.6 for SSP1-1.9 (Fig. 5e). These changes reflect increases in the year-to-year variability of precipitation maxima with warming ^{84,98} and increases in the daily area fraction receiving precipitation ⁹⁹, both linked to ongoing increases in the water-holding capacity of the atmosphere ¹⁰⁰. Yet, these thermodynamically driven changes can be strongly modified by changes in atmospheric dynamics regionally and seasonally ¹⁰¹, particularly in the subtropics where signals can even be reversed ¹⁰². Over most extratropical land regions, a robust increase in the intensity of annual extreme precipitation is projected ⁸⁰.

At smaller spatial scales, any long-term signals in extreme precipitation records are increasingly influenced by very large unforced internal variability ¹⁰³⁻¹⁰⁶. As such, record local rainfall levels do not often follow a gradual smooth increase, but rather step-like changes: clustered years of record-breaking events, some by a considerable margin, followed by a long pause in which the record level does not increase ¹⁰³. For example, there is clear evidence towards more intense extreme rainfall events over the UK as a whole (Fig. 6a), but when examined

locally, record-breaking events could be followed by surprisingly long periods, even up to multiple decades, when no new records are set (Fig. 6b). Thus, changes in record-breaking probability become more apparent after aggregating records over sufficiently large regions or time periods.

Increases in the frequency of record drought across global land regions are also projected in the future. Indeed, by the end of the twenty-first century, multimodel mean record ratios for monthly record dryness (P–E) over land are -3.1 for SP5-8.5, -2.7 for SSP3-7.0, -2.1 for SSP2-4.5, -1.6 for SSP1-2.6 and -1.2 for SSP1-1.9 (Fig. 5f). Similar to the heavy precipitation, scenarios tend to follow roughly the same trajectory towards 2050 and diverge thereafter.

Record behaviour across the climate system

Record-breaking events are not limited to temperature or rainfall. In principle, they can occur for any climate variable for which there is a pronounced thermodynamic contribution from climate change. However, although individual record-breaking events have been reported (for example, for geopotential height and the elevation of the zero degree line ¹⁰⁷), characterization of record statistics is limited outside temperature and precipitation owing to data concerns (absence, length and inhomogeneities). Evidence of record behaviour in other parts of the climate system is now discussed, focusing on ice sheets, glaciers, sea ice, ocean heat content and sea level, although records are prevalent across many other components too.

Record behaviour has been observed for Greenland Ice Sheet (GrIS) and Antarctic Ice Sheet (AIS) mass loss. Although experiencing large interannual variability, signals are integrated across the ice sheets (owing to their size and inertia) to provide a high signal-to-noise ratio. Before 2000, the GrIS was relatively balanced year to year, with a net cumulative change of near zero. Every year since, however, has witnessed record values of cumulative ice mass loss 108,109, corresponding to a 13.6 mm contribution to global sea-level rise from the GrIS by 2021. Relatedly, all years from 2000 until 2013 have experienced runoff that is outside the range of reconstructed runoff for the previous 200 years of 225 ± 26 Gt per year ¹¹⁰, including three record runoff years in 2003 (352 Gt per year), 2011 (378 Gt per year) and 2012 (389 Gt per year). Ice discharge (ice lost by calving) has also been increasing, with record discharge rates in 9 of the years since 2010 and a maximum value of 507 Gt per year in 2021 (ref. 111). Accumulation has only increased marginally during this time, meaning records related to mass loss can be expected to increase as warming continues 110,112. For the AIS, most mass loss can be attributed to basal melting below the floating ice shelves, as there is not yet a clear trend in the surface forcing 113 or a strong trend in discharge 114 . The AIS is, nonetheless, losing mass at a high rate, leading to record values of cumulative mass loss every year and a contribution to global sea-level rise of 7.4 mm by 2021 (ref. 108).

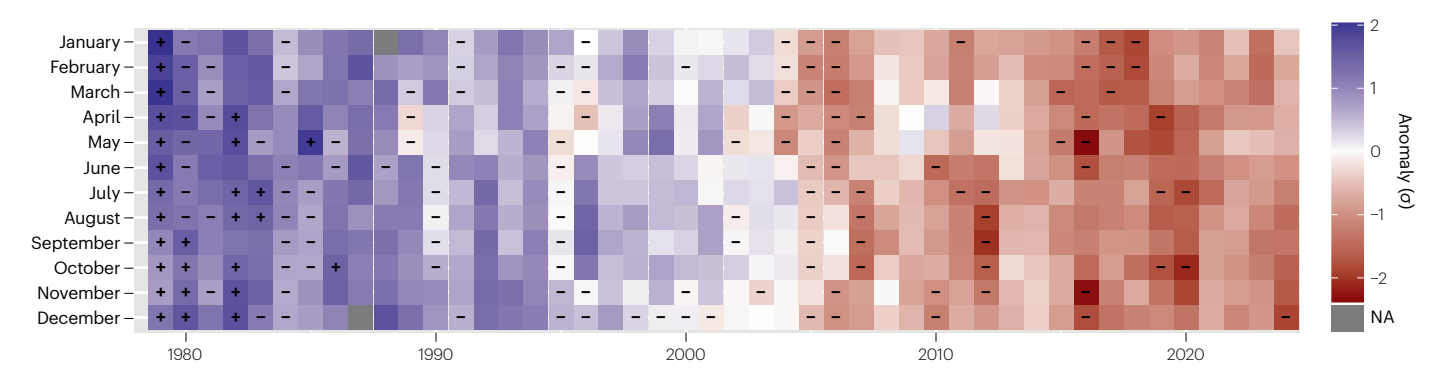
As in Greenland and Antarctica, there is observational evidence for record mass loss in mountain glaciers around the world. In the Southern Alps of New Zealand, for example, record-high mass loss was observed in 2011 and 2019 (refs. 115,116). Similarly, record glacial loss occurred in the European Alps in 2022 (ref. 117), including in Switzerland which experienced the greatest annual ice mass loss since the beginning of measurements (as also in 2023) with 10% of the total glacier volume lost in only 2 years¹¹⁸.

Looking beyond land ice, record minima have occurred for sea ice in both the Arctic and the Antarctic. For example, Arctic sea ice extent (SIE) experienced 93 monthly record minima between 1979 and 2020 (ref. 119), roughly 6–8 times more record minima than expected without climate change (Fig. 7). Prominent sea ice minima occurred in 2005, 2007 and 2012 and have been related to anomalous atmospheric circulation patterns and excess solar radiation absorbed by open ocean 120–125. Conversely, there has been no single monthly record maximum Arctic SIE since 1986 (refs. 119,126) (Fig. 7). Antarctic SIE has not experienced a comparable long-term decline 127. Instead, there were 3 consecutive years with record high Antarctic SIE in 2012, 2013 and peaking in September 2014 with 20.2 million km² (ref. 119). These record maxima were followed by a series of record minima after 2017 (refs. 128–130), with the lowest Antarctic SIE of 1.77 million km² reached in February 2023 (ref. 131).

Records are also being broken in the ocean. Beyond SST, record high global ocean heat (OHC) has been observed since 1955 (ref. 132). For instance, at least 17 of the years since 2000 have seen record annual mean OHC values, culminating in a peak in 2023 and 2024. Given that the OHC time series has roughly been following a linear positive trend since the late 1980s and variability is low, the large proportion of records can be expected to continue. Moreover, cumulative increases in ice mass loss and OHC (and thereby thermal expansion) also contribute to regular record sea levels 127,133,134. The positive trend in sea level has primed the system for record flooding and storm-surge events 135.

Anticipating record events for adaptation

Record-breaking and record-shattering extremes often have large impacts on society, economy and ecosystems. Their impacts can be



 $mean \ and \ standard \ deviation. \ Record \ high \ and \ low \ values for the corresponding month are marked \ with + and -, respectively. \ Plenty of record \ minima \ in \ Arctic sea ice extent has been observed since 1984, but no record \ maxima. \ NA, not available.$

so substantial because planning efforts often primarily rely on the observational record. Thus, depending on how well the possibility of a large record margin was quantified or how large the safety margins in planning were, the vulnerability to such events, unprecedented in the observational record, could be particularly large. These events, therefore, necessitate and drive adaptation. For instance, in the aftermath of a record-shattering event, governments and individuals usually act quickly to reduce risk through short-termadaptation 136-138. But to proactively adapt before (rather than after) record-breaking events, reliable information on potential future events is crucial, particularly given projected increases in the population exposed to such extremes 139.

Physical climate storylines provide one such opportunity. In addition to probabilistic return level estimations¹⁴⁰, these storylines anticipate the potential intensity, duration or spatial extent of future record-shattering events¹⁴¹⁻¹⁴⁵. The approaches to develop event storylines include statistical methods, such as empirical importance sampling, in which statistical weather generators use atmospheric flow analogues from reanalysis to sample very extreme and persistent sequences of weather patterns (including persistent blocking anticyclones conducive to heatwaves) 144,146,147. Other approaches are based on searching large ensembles of initialized weather forecasts from numerical weather prediction models and subseasonal to seasonal or decadal prediction systems for very extreme weather and climate events^{145,148-150}. Such events that were predicted based on observed atmospheric states but never materialized in reality might provide guidance on plausible high return level events that could happen under today's conditions.

Although the aforementioned approaches benefit from historical evidence used for constructing analogues or initializing models, they could potentially be overly conservative in cases in which unseen conditions in the oceans and land emerge, which have not occurred in the past. Thus, plausible very high return events can also be searched for in multimodel or single-model initial condition large ensembles of fully coupled Earth system models that sample ocean states that have not been observed in recent decades. Earth system models can also be used as a tool to specifically search for potential worst-case events using rare event algorithms ^{142,151} or ensemble boosting ^{143,152}. In rare event algorithms, a climate model is perturbed and the most extreme model trajectories are selected and perturbed again. This process is repeated to simulate very extreme events and calculate their probability 142,151 . In ensemble boosting, the most extreme events from a long simulation are selected and the corresponding simulations are re-initialized with random perturbations to specifically sample the tail of the model distribution. Such tools can be used to inform and develop physical climate storylines that characterize the spatial extent, intensity and time evolution for potential future record-shattering extremes. Each of these different tools has strengths and weaknesses and involves substantial uncertainties. Thus, ideally the lines of evidence from different tools are combined to produce robust climate information for decision-making. Independent of the approach, it is vital to take into account that the current level of warming, and in many regions the rate of warming is unprecedented in the observational record.

A comprehensive climate risk assessment needs to account for low-likelihood high-impact events. Such low-likelihood high-impact events can occur from single rare events or events that arise from unlikely combinations of factors, processes or even events. Tipping points are one such example, in which the system crosses a threshold. Also, events that used to be very rare might occur more frequently in the future, perhaps in combination as compound events, cluster within

short time periods or co-occur in space, amplifying their impacts. However, impacts are not purely consequences of the physical climate hazards but also of exposure and vulnerability that can be partly reduced through adaptation. Storylines are tools that allow us to explore these potential chains of causal factors that can lead to low-likelihood high-impact events and worst-case scenarios¹⁵³.

In all storyline approaches, the plausibility of the estimated record-shattering and unprecedented events needs to be carefully evaluated. For example, potential physical mechanisms leading to such extreme events in weather and climate models must be investigated, and their impacts compared with more moderate observed events. Once plausibility is sufficiently evaluated, such approaches can become powerful tools for stress testing the resilience of flood protection measures, public health plans, energy grids or food security to record-shattering extremes.

Summary and future perspectives

Statistically, the behaviour of record-breaking and record-shattering extremes is well understood, and their probability is directly related to the signal-to-noise ratio. Changes in the occurrence of record-breaking climate events is simply and usefully captured by the record ratio relative to a stationary climate. Indeed, the assessment of record ratios indicates that climate change has altered, and will continue to alter the occurrence of record-breaking and record-shattering events across the climate system. For example, on land, all-time daily hot records, annual 1-day maximum precipitation records and monthly dryness (P-E) records are ~4.1 (Fig. 3a), ~1.4 (Fig. 5a) and ~1.12 (Fig. 5c) times more frequent now (2016-2024) than expected in a stationary climate, respectively; all-time daily cold records are less than half as frequent (Fig. 3a). There are also clear observed signals of climate change in the record behaviour of low Arctic sea ice extent, melting glaciers and ice sheets. These changes directly relate to the high rate of forced warming, which will yield more record-shattering records in coming years as many places have not yet experienced anything close to the most intense extremes expected in the coming decades. Indeed, with ongoing warming (based on SSP3-7.0), record ratios by the end of the twenty-first century could reach ~15.7 for all-time daily heat (Fig. 4a), nearly 0 for all-time daily cold (Fig. 4b), ~4.3 for 1-day maximum precipitation (Fig. 5e) and ~2.7 for monthly dryness (Fig. 5f). Emissions reductions and thereby a slowing of the forced warming trend would offer early benefits by rapidly reducing record ratios across many climate variables.

Despite in-depth knowledge about these record-breaking events, substantial knowledge gaps and challenges remain. Data availability is one such limitation. Robustly quantifying the occurrence of record-breaking events requires long, homogeneous observational records or reanalyses. Yet, a lack of appropriate data, inhomogeneities or gaps in the observational records and internal variability all hinder or limit record statistics. Efforts to continue coherent observational and monitoring networks, to develop observational networks in many data-sparse regions (such as parts of Africa), to rescue data from historical archives and to homogenize data will thus be particularly valuable for the monitoring of record-breaking extremes. Large multimodel and initial condition ensembles have become an important additional tool and add to the understanding of record events, but they also need to be carefully evaluated against observational products. Machine-learning-based methods, augmenting existing highresolution climate model experiments, could allow better sampling of record-breaking events¹⁵⁴.

From a statistical perspective, there are appropriate knowledge and tools to assess record events in the univariate case. However, there is a need to extend some of these frameworks to multivariate records that are relevant to compound climate events, including spatially co-occurring records, record-breaking clustering of events or compound records such as combined drought and heat or combined wind, extreme precipitation and storm surge. If compound events relate to multiple variables that are affected by climate change, records might change particularly rapidly in a warming climate. To this end, it is essential to adequately account for the dependence structure across variables and potential changes thereof in a warming climate. This point could be achieved by exploiting modelling approaches from the statistics of multivariate and/or spatial extremes 155,156 and letting dependence parameters evolve over time according to a range of climate change scenarios 157,158.

Further efforts are also needed to understand and quantify plausible intensities of future record-shattering or worst-case events in the near future. Quantitative methods such as the use of rare event algorithms, weather generators, ensemble boosting or targeted exploration of initialized hindcasts are promising first steps. These methods can be complemented by qualitative process-based storylines, in which narratives of worst-case scenarios are developed using the understanding of causal factors and plausible combinations of these.

In addition to the development of physical climate storylines. more research is needed on how adaptation and planning can take into account potential large record margins and novel combinations of compound record-breaking events. Strengthening resilience can be performed across different layers ranging from addressing immediate threats through improved short-term disaster preparedness to transformative adaptation enhancing long-term resilience¹⁵⁹.

Extreme anomalies occur randomly by chance. Nevertheless, there have been first attempts to quantify where the most intense record-shattering extremes could occur. This quantification can be done by evaluating where the current record level in observations most strongly deviates from a high return level^{29,152}. Following statistical considerations (Fig. 2), it is clear that the forced warming rate and potential changes in variability, which can be estimated from observations, reanalysis or model experiments, are important factors in quantifying the probability of experiencing record-shattering extremes.

The large number of record-breaking extremes, their very large record margins and often large impacts on society, economy and ecosystems highlight the need for greater attention from the science community. Evidence from statistical considerations and model experiments explains why the probability of such events is higher today and compared with a stationary climate. To increase resilience and better prepare for future events, it will be crucial to combine different statistical and model-based tools, develop storylines of weather and climate extremes and their impacts and closely collaborate across the many relevant science disciplines.

Published online: 29 May 2025

References

- Bartusek, S., Kornhuber, K. & Ting, M. 2021 North American heatwave amplified by climate change-driven nonlinear interactions. Nat. Clim. Change https://doi.org/10.1038/ s41558-022-01520-4 (2022).
- McKinnon, K. A. & Simpson, I. R. How unexpected was the 2021 Pacific Northwest heatwave? Geophys. Res. Lett. 49, e2022GL100380 (2022).
- Schumacher, D. L., Hauser, M. & Seneviratne, S. I. Drivers and mechanisms of the 2021 Pacific Northwest heatwave. Earth's Future 10, e2022EF002967 (2022).
- White, R. H. The unprecedented Pacific Northwest heatwave of June 2021, Nat. Commun.

- Overland, J. E. & Wang, M. The 2020 Siberian heat wave. Int. J. Climatol. 41, 2341-2346
- Ciavarella, A. et al. Prolonged Siberian heat of 2020 almost impossible without human influence. Clim. Change 166, 9 (2021).
- Characteristics and causes of the hot-dry climate anomalies in China during summer of 2022. Trans. Atmos. Sci. 46, 1-8 (2023).
- Jiang, J., Liu, Y., Mao, J. & Wu, G. Extreme heatwave over eastern China in summer 2022: the role of three oceans and local soil moisture feedback. Environ. Res. Lett. 18, 044025 (2023)
- Yule, E. L., Hegerl, G., Schurer, A. & Hawkins, E. Using early extremes to place the 2022 UK heat waves into historical context, Atmos. Sci. Lett. 24, e1159 (2023).
- 10. Barriopedro, D., Fischer, E. M., Luterbacher, J., Trigo, R. & Garcia-Herrera, R. The hot summer of 2010; redrawing the temperature record map of Europe. Science 332. 220-224 (2011).
- Miralles D.G. Teuling A. I. & Heerwaarden, C. C. V. Mega-heatwaye temperatures due to combined soil desiccation and atmospheric heat accumulation, Nat. Geosci. 7, 345-349 (2014)
- Fischer, E. M. Climate science: autopsy of two mega-heatwaves. Nat. Geosci. 7, 332-333 (2014)
- 13. Bador, M. et al. Future summer mega-heatwave and record-breaking temperatures in a warmer France climate. Environ. Res. Lett. 12, 074025 (2017).
- Cadiou, C., Noyelle, R., Malhomme, N. & Faranda, D. Challenges in attributing the 2022 Australian rain bomb to climate change. Asia-Pacific J. Atmos. Sci. 59, 83-94 (2023).
- 15. Malik, I., Chuphal, D. S., Vegad, U. & Mishra, V. Was the extreme rainfall that caused the August 2022 flood in Pakistan predictable? Environ. Res. Clim. 2, 041005 (2023).
- Ma, Y. et al. Different characteristics and drivers of the extraordinary Pakistan rainfall in July and August 2022. Remote Sens. 15, 2311 (2023).
- Nanditha, J. S. et al. The Pakistan flood of August 2022: causes and implications. Earth's Future 11, e2022EF003230 (2023).
- Tradowsky, J. S. et al. Attribution of the heavy rainfall events leading to severe flooding in western Europe during July 2021. Clim. Change 176, 90 (2023).
- Robine, J. M. et al. Death toll exceeded 70,000 in Europe during the summer of 2003. Comptes rendus Biol. 331, 171-178 (2008)
- Garca-Herrera, R., Daz, J., Trigo, R. M., Luterbacher, J. & Fischer, E. M. A review of the European summer heat wave of 2003. Crit. Rev. Environ. Sci. Technol. 40, 267-306
- 21. Kirsch, T. D., Wadhwani, C., Sauer, L., Doocy, S. & Catlett, C. Impact of the 2010 Pakistan floods on rural and urban populations at six months, PLoS Curr. 4, e4fdfb212d2432 (2012)
- Cassola, F., lengo, A. & Turato, B. Extreme convective precipitation in Liguria (Italy): a brief description and analysis of the event occurred on October 4, 2021, Bull, Atmos. Sci. Technol. 4, 4 (2023).
- Wille, J. D. et al. The extraordinary March 2022 East Antarctica 'heat' wave. Part I: observations and meteorological drivers. J. Clim. 37, 757-778 (2024). https://journals. ametsoc.org/view/iournals/clim/37/3/JCLI-D-23-0175.1.xml.
- Meehl, G. A., Tebaldi, C., Walton, G., Easterling, D. & McDaniel, L. Relative increase of record high maximum temperatures compared to record low minimum temperatures in the U.S. Geophys, Res. Lett. 36, L23701 (2009).
- Elguindi, N., Rauscher, S. A. & Giorgi, F. Historical and future changes in maximum and minimum temperature records over Europe. Clim. Change 117, 415-431 (2013)
- Bador, M., Terray, L. & Boé, J. Detection of anthropogenic influence on the evolution of record-breaking temperatures over Europe. Clim. Dyn. 46, 2717-2735 (2016).
- Sena, E. T., Koren, I., Altaratz, O. & Kostinski, A. B. Record-breaking statistics detect islands of cooling in a sea of warming. Atmos. Chem. Phys. 22, 16111-16122 (2022).
- Fischer, E. M., Sippel, S. & Knutti, R. Increasing probability of record-shattering climate extremes. Nat. Clim. Change 11, 689-695 (2021).
- Thompson, V. et al. The most at-risk regions in the world for high-impact heatwaves Nat. Commun. 14, 2152 (2023).
- de Vries, I., Sippel, S., Zeder, J., Fischer, E. & Knutti, R. Increasing extreme precipitation variability plays a key role in future record-shattering event probability. Commun. Earth Environ. 5, 482 (2024)
- Lehmann, J., Coumou, D. & Frieler, K. Increased record-breaking precipitation events under global warming. Clim. Change 132, 501-515 (2015).
- Lehmann, J., Mempel, F. & Coumou, D. Increased occurrence of record-wet and record-dry months reflect changes in mean rainfall. Geophys. Res. Lett. 45, 13-468 (2018).
- 33. Bassett, G. W. Breaking recent global temperature records. Clim. Change 21, 303-315 (1992).
- 34 Holden, C. Watch out! Here comes the greenhouse, Science 248, 549-549 (1990).
- Glick, N. Breaking records and breaking boards. Am. Math. Monthly 85, 2-26 (1978). 35.
- Resnick, S. Extreme Values, Regular Variation, and Point Processes (Springer, 1987). 36
- Davison, A. C. & Huser, R. Statistics of extremes, Annu. Rev. Stat. Appl. 2, 203-235 (2015). 37.
- Galambos. J. The Asymptotic Theory of Extreme Order Statistics 2nd edn (Krieger, 1987). 38.
- Arnold, B. C., Balakrishnan, N. & Nagaraja, H. N. Records (Wiley, 1998). 39.
- Benestad, R. E. How often can we expect a record event? Clim. Res. 25, 3-13 (2003). 40
- 41. Benestad, R. E. Record-values, nonstationarity tests and extreme value distributions. Glob, Planet, Change 4, 11-26 (2004).
- Wergen, G. & Krug, J. Record-breaking temperatures reveal a warming climate. Europhys. Lett. 92, 30008 (2010).

- Rahmstorf, S. & Coumou, D. Increase of extreme events in a warming world. Proc. Natl Acad. Sci. USA 108, 17905–17909 (2011).
- Falk, M., Khorrami Chokami, A. & Padoan, S. A. Records for time-dependent stationary Gaussian sequences. J. Appl. Probab. 57, 78–96 (2020).
- Naveau, P. et al. Revising return periods for record events in a climate event attribution context. J. Clim. 31, 3411–3422 (2018).
- Worms, J. & Naveau, P. Record events attribution in climate studies. Environmetrics 33, e2777 (2022).
- Gonzalez, P., Naveau, P., Thao, S. & Worms, J. A statistical method to model non-stationarity in precipitation records changes. Geophys. Res. Lett. 52, e2023GL107201 (2023).
- Rodgers, K. B. et al. Ubiquity of human-induced changes in climate variability. Earth Syst. Dyn. 12, 1393–1411 (2021).
- Zscheischler, J. & Fischer, E. M. The record-breaking compound hot and dry 2018 growing season in Germany. Weather Clim. Extremes 29, 100270 (2020).
- Castruccio, S., Huser, R. & Genton, M. G. High-order composite likelihood inference for max-stable distributions and processes. J. Comput. Graph. Stat. 25, 1212–1229 (2016)
- Bador, M., Terray, L. & Boé, J. Emergence of human influence on summer record-breaking temperatures over Europe. Geophys. Res. Lett. 43, 404–412 (2016).
- Rohde, R. A. & Hausfather, Z. The Berkeley Earth land/ocean temperature record. Earth Syst. Sci. Data 12, 3469–3479 (2020).
- Coumou, D., Robinson, A. & Rahmstorf, S. Global increase in record-breaking monthly-mean temperatures. Clim. Change 118, 771–782 (2013).
- Robinson, A., Lehmann, J., Barriopedro, D., Rahmstorf, S. & Coumou, D. Increasing heat and rainfall extremes now far outside the historical climate. npj Clim. Atmos. Sci. 4, 45 (2021).
- Wergen, G. & Krug, J. Record-breaking temperatures reveal a warming climate. epl 92, 30008 (2010).
- Newman, W. I., Malamud, B. D. & Turcotte, D. L. Statistical properties of record-breaking temperatures. *Phys. Rev. E* 82, 66111 (2010).
- Ruokolainen, L. & Räisänen, J. How soon will climate records of the 20th century be broken according to climate model simulations? *Tellus A* 61, 476–490 (2009).
- Christiansen, B. Changes in temperature records and extremes: are they statistically significant? J. Clim. 26, 7863–7875. http://journals.ametsoc.org/doi/abs/10.1175/ JCLI-D-12-00814.1.
- Wergen, G., Hense, A. & Krug, J. Record occurrence and record values in daily and monthly temperatures. Clim. Dyn. 42, 1275–1289 (2014).
- Holbrook, N. J. et al. Keeping pace with marine heatwaves. Nat. Rev. Earth Environ. 1, 482–493 (2020).
- 61. Oliver, E. C. et al. Marine heatwaves. Annu. Rev. Mar. Sci. 13, 313-342 (2021).
- Frölicher, T. L., Fischer, E. M. & Gruber, N. Marine heatwaves under global warming. Nature 560, 360–364 (2018).
- Pan, Z., Wan, B. & Gao, Z. Asymmetric and heterogeneous frequency of high and low record-breaking temperatures in China as an indication of warming climate becoming more extreme. J. Geophys. Res. Atmospheres 118, 6152–6164 (2013).
- Mueller, N. D. et al. Cooling of US Midwest summer temperature extremes from cropland intensification. Nat. Clim. Change 6, 317–322 (2016).
- Singh, J., Sippel, S. & Fischer, E. M. Circulation dampened heat extremes intensification over the Midwest USA and amplified over western Europe. Commun. Earth Environ. 4, 432 (2023).
- Evolution and distribution of record-breaking high and low monthly mean temperatures.
 J. Appl. Meteorol. Climatol. 50, 1859–1871 (2011).
- Rowe, C. M. & Derry, L. E. Trends in record-breaking temperatures for the conterminous United States. Geophys. Res. Lett. https://doi.org/10.1029/2012GL052775 (2012).
- Dramatically increased rate of observed hot record breaking in recent Australian temperatures. Geophys. Res. Lett. 42, 7776–7784 (2015).
- Lorenz, R., Stalhandske, Z. & Fischer, E. Detection of a climate change signal in extreme heat, heat stress, and cold in Europe from observations. Geophys. Res. Lett. 46, 8363–8374 (2019).
- Rousi, E., Kornhuber, K., Beobide-Arsuaga, G., Luo, F. & Coumou, D. Accelerated western European heatwave trends linked to more-persistent double jets over Eurasia. *Nat. Commun.* 13, 3851 (2022).
- Vautard, R. et al. Heat extremes in western Europe increasing faster than simulated due to atmospheric circulation trends. Nat. Commun. 14, 6803 (2023).
- Schumacher, D. L. et al. Exacerbated summer European warming not captured by climate models neglecting long-term aerosol changes. Commun. Earth Environ. 5, 182 (2024).
- King, A. D., Oldenborgh, G. J. V., Karoly, D. J., Lewis, S. C. & Cullen, H. Attribution of the record high Central England temperature of 2014 to anthropogenic influences. *Environ. Res. Lett.* 10, 054002 (2015).
- Beniston, M. Ratios of record high to record low temperatures in Europe exhibit sharp increases since 2000 despite a slowdown in the rise of mean temperatures. Clim. Change https://doi.org/10.1007/s10584-015-1325-2 (2015).
- Trewin, B. & Vermont, H. Changes in the frequency of record temperatures in Australia, 1957–2009. Aust. Meteorol. Oceanogr. J. 60, 113–119 (2010).
- Doblas-Reyes, F. et al. Linking global to regional climate change. In Climate Change 2021: Physical Science Basis. Contribution of Working Group I to the Sixth Assessment Report of the Intergovernmental Panel on Climate Change, 1363–1512 (Cambridge Univ. Press, 2021).

- Gross, M. H., Donat, M. G., Alexander, L. V. & Sherwood, S. C. Amplified warming of seasonal cold extremes relative to the mean in the Northern Hemisphere extratropics. *Earth Syst. Dyn.* 11, 97–111 (2020).
- Screen, J. A. Arctic amplification decreases temperature variance in northern mid-to high-latitudes. Nat. Clim. Change 4, 577–582 (2014).
- Blackport, R., Fyfe, J. C. & Screen, J. A. Decreasing subseasonal temperature variability in the northern extratropics attributed to human influence. Nat. Geosci. 14, 719–723 (2021).
- 80. Seneviratne, S. et al. Weather and climate extreme events in a changing climate. In Climate Change 2021: Physical Science Basis. Contribution of Working Group to the Sixth Assessment Report of the Intergovernmental Panel on Climate Change (2021).
- Zorita, E., Stocker, T. & von Storch, H. How unusual is the recent series of warm years? Geophys. Res. Lett. https://doi.org/10.1029/2008GL036228 (2008).
- 82. King, A. D. Attributing changing rates of temperature record breaking to anthropogenic influences. *Earth's Future* **5**, 1156–1168 (2017).
- Power, S. B. & Delage, F. P. Setting and smashing extreme temperature records over the coming century. Nat. Clim. Change 9, 529–534 (2019).
- Pendergrass, A. G., Knutti, R., Lehner, F., Deser, C. & Sanderson, B. M. Precipitation variability increases in a warmer climate. Sci. Rep. 7, 17966 (2017).
- 85. Matte, D. et al. On the potentials and limitations of attributing a small-scale climate event. *Geophys. Res. Lett.* **49**, e2022GL099481 (2022).
- 86. Golding, B., Clark, P. & May, B. The Boscastle flood: meteorological analysis of the conditions leading to flooding on 16 August 2004. Weather **60**, 230–235 (2005).
- Wu, P. et al. A case study of the July 2021 Henan extreme rainfall event: from weather forecast to climate risks. Weather Clim. Extremes 40, 100571 (2023).
- 88. Kendon, M. & McCarthy, M. The United Kingdom's wettest day on record so far 3 October 2020. Weather **76**, 316–319 (2021).
- Hohenegger, C., Walser, A., Langhans, W. & Schär, C. Cloud-resolving ensemble simulations of the August 2005 Alpine flood. Q. J. R. Meteorol. Soc. 134, 889–904 (2008).
- Kendon, E. J., Blenkinsop, S. & Fowler, H. J. When will we detect changes in short-duration precipitation extremes? J. Clim. 31, 2945–2964 (2018).
- Contractor, S. et al. Rainfall estimates on a gridded network (REGEN) a global land-based gridded dataset of daily precipitation from 1950 to 2016. Hydrol. Earth Syst. Sci. 24, 919–943 (2020).
- 92. Büntgen, U. et al. Recent European drought extremes beyond common era background variability. *Nat. Geosci.* **14**, 190–196 (2021).
- Williams, A. P., Cook, B. I. & Smerdon, J. E. Rapid intensification of the emerging southwestern North American megadrought in 2020–2021. Nat. Clim. Change 12, 232–234 (2022).
- Brunner, M. I., Liechti, K. & Zappa, M. Extremeness of recent drought events in Switzerland: dependence on variable and return period choice. Nat. Hazards Earth Syst. Sci. 19, 2311–2323 (2019)
- Ionita, M., Dima, M., Nagavciuc, V., Scholz, P. & Lohmann, G. Past megadroughts in Central Europe were longer, more severe and less warm than modern droughts. Commun. Earth Environ. 2, 61 (2021).
- Marvel, K. et al. Twentieth-century hydroclimate changes consistent with human influence. Nature 569, 59–65 (2019).
- Bonfils, C. J. et al. Human influence on joint changes in temperature, rainfall and continental aridity. Nat. Clim. Change 10, 726–731 (2020).
- 98. Zhang, W. et al. Increasing precipitation variability on daily-to-multiyear time scales in a warmer world. Sci. Adv. 7, eabf8021 (2021).
- Benestad, R. E., Lussana, C. & Dobler, A. A link between the global surface area receiving daily precipitation, wet-day frequency and probability of extreme rainfall. *Discov. Water* 4, 10 (2024).
- 100. Douville, H. et al. Water cycle changes. In Climate Change 2021: The Physical Science Basis. Contribution of Working Group I to the Sixth Assessment Report of the Intergovernmental Panel on Climate Change, 1055–1210 (Cambridge Univ. Press, 2021).
- Bador, M. & Alexander, L. V. Future seasonal changes in extreme precipitation scale with changes in the mean. Earth's Future 10, e2022EF002979 (2022).
- Pfahl, S., O'Gorman, P. & Fischer, E. Understanding the regional pattern of projected future changes in extreme precipitation. Nat. Clim. Change 7, 423–427 (2017).
- Kendon, E. J., Fischer, E. M. & Short, C. J. Variability conceals emerging trend in 100yr projections of UK local hourly rainfall extremes. *Nat. Commun.* 14, 1133 (2023).
- 104. Fischer, E. M., Beyerle, U. & Knutti, R. Robust spatially aggregated projections of climate extremes. Nat. Clim. Change 3, 1033–1038 (2013).
- 105. Aalbers, E. E., Lenderink, G., van Meijgaard, E. & van den Hurk, B. J. Local-scale changes in mean and heavy precipitation in western Europe, climate change or internal variability? Clim. Dyn. 50, 4745–4766 (2018).
- Hawkins, E. & Sutton, R. The potential to narrow uncertainty in projections of regional precipitation change. Clim. Dyn. 37, 407–418 (2010).
- Scherrer, S. C., Gubler, S., Wehrli, K., Fischer, A. M. & Kotlarski, S. The Swiss Alpine zero degree line: methods, past evolution and sensitivities. *Int. J. Climatol.* 41, 6785–6804 (2021).
- Otosaka, I. N. et al. Mass balance of the Greenland and Antarctic ice sheets from 1992 to 2020. Earth Syst. Sci. Data 15, 1597–1616 (2023).
- 109. Mass balance of the Greenland ice sheet from 1992 to 2018. *Nature* **579**, 233–239 (2020). 110. Trusel, L. D. et al. Nonlinear rise in Greenland runoff in response to post-industrial Arctic
- warming. Nature **564**, 104–108 (2018).
- Mankoff, K. D. et al. Greenland ice sheet mass balance from 1840 through next week. Earth Syst. Sci. Data Discuss. 2021, 1–37 (2021).

- 112. Fettweis, X. et al. Estimating the Greenland ice sheet surface mass balance contribution to future sea level rise using the regional atmospheric climate model MAR. Cryosphere 7, 469–489 (2013).
- Mottram, R. et al. What is the surface mass balance of Antarctica? An intercomparison of regional climate model estimates. Cryosphere 15, 3751–3784 (2021).
- 114. Noël, B. et al. Higher Antarctic ice sheet accumulation and surface melt rates revealed at 2 km resolution. Nat. Commun. 14, 7949 (2023).
- Vargo, L. J. et al. Anthropogenic warming forces extreme annual glacier mass loss. Nat. Clim. Change 10, 856–861 (2020).
- Hugonnet, R. et al. Accelerated global glacier mass loss in the early twenty-first century. Nature 592, 726–731 (2021).
- Voordendag, A., Prinz, R., Schuster, L. & Kaser, G. Brief communication: the glacier loss day as an indicator of a record-breaking negative glacier mass balance in 2022. Cryosophere 17, 3661–3665 (2023).
- Huss, M. The Alps' iconic glaciers are melting, but there's still time to save the biggest. Bull. At. Scientists 80, 225–229 (2024).
- Parkinson, C. L. & DiGirolamo, N. E. Sea ice extents continue to set new records: Arctic, Antarctic, and global results. Remote Sens. Environ. 267, 112753 (2021).
- Zhang, J., Lindsay, R., Schweiger, A. & Steele, M. The impact of an intense summer cyclone on 2012 Arctic sea ice retreat. Geophys. Res. Lett. 40, 720-726 (2013).
- 121. Stroeve, J. et al. Arctic sea ice extent plummets in 2007. EOS 89, 13-14 (2008).
- Schweiger, A. J., Zhang, J., Lindsay, R. W. & Steele, M. Did unusually sunny skies help drive the record sea ice minimum of 2007? Geophys. Res. Lett. https://doi.org/10.1029/ 2008GL033463 (2008).
- Kauker, F. et al. Adjoint analysis of the 2007 all time Arctic sea-ice minimum. Geophys. Res. Lett. https://doi.org/10.1029/2008GL036323 (2009).
- Perovich, D. K., Richeter-Menge, J. A., Jones, K. F. & Light, B. Sunlight, water, and ice: extreme Arctic sea ice melt during the summer of 2007. Geophys. Res. Lett. https://doi.org/10.1029/2008GL034007 (2008).
- Kay, J. E. & Gettelman, A. Cloud influence on and response to seasonal Arctic sea ice loss. J. Geophys. Res. Atmos. https://doi.org/10.1029/2009JD011773 (2009).
- Parkinson, C. L. & DiGirolamo, N. E. New visualizations highlight new information on the contrasting Arctic and Antarctic sea-ice trends since the late 1970s. Remote Sens. Environ. 183, 198–204 (2016).
- 127. Fox-Kemper, B. et al. Ocean, cryosphere, and sea level change. In Climate Change 2021: Physical Science Basis. Contribution of Working Group I to the Sixth Assessment Report of the Intergovernmental Panel on Climate Change, 1211–1361 (Cambridge Univ. Press, 2021).
- Zhang, C. & Li, S. Causes of the record-low Antarctic sea-ice in austral summer 2022.
 Atmos. Ocean. Sci. Lett. 16, 100353 (2023).
- Wang, J. et al. An unprecedented record low Antarctic sea-ice extent during austral summer 2022. Adv. Atmos. Sci. 39, 1591–1597 (2022).
- Liu, J., Zhu, Z. & Chen, D. Lowest Antarctic sea ice record broken for the second year in a row. Ocean Land Atmos. Res. 2, 0007 (2023).
- 131. Purich, A. & Doddridge, E. W. Record low Antarctic sea ice coverage indicates a new sea ice state. Commun. Earth Environ. 4, 314 (2023).
- Cheng, L. et al. Another year of record heat for the oceans. Adv. Atmos. Sci. 40, 963–974 (2023).
- Church, J. A. & White, N. J. Sea-level rise from the late 19th to the early 21st century. Surv. Geophys. 32, 585–602 (2011).
- 134. Frederikse, T. et al. The causes of sea-level rise since 1900. Nature **584**, 393-397 (2020).
- 135. Taherkhani, M. et al. Sea-level rise exponentially increases coastal flood frequency. Sci. Rep. **10**, 6466 (2020).
- 136. Finucane, M. L., Acosta, J., Wicker, A. & Whipkey, K. Short-term solutions to a long-term challenge: rethinking disaster recovery planning to reduce vulnerabilities and inequities. *Int. J. Environ. Res. Public Health* 17, 482 (2020).
- 137. O'Neill, B. C. et al. Key risks across sectors and regions. In Climate Change 2022: Impacts, Adaptation and Vulnerability. Contribution of Working Group II to the Sixth Assessment Report of the Intergovernmental Panel on Climate Change, 2411–2538 (Cambridge Univ. Press, 2022).
- Kirchhoff, C. J. & Watson, P. L. Are wastewater systems adapting to climate change?
 J. Am. Water Resour. Assoc. 55, 869–880 (2019).
- Li, B. et al. Future global population exposure to record-breaking climate extremes. Earth's Future 11, e2023EF003786 (2023).
- Zeder, J., Sippel, S., Pasche, O. C., Engelke, S. & Fischer, E. M. The effect of a short observational record on the statistics of temperature extremes. *Geophys. Res. Lett.* 50, e2023GL104090 (2023).
- Schaller, N. et al. The role of spatial and temporal model resolution in a flood event storyline approach in western Norway. Weather Clim. Extremes 29, 100259 (2020).
- Ragone, F. & Bouchet, F. Rare event algorithm study of extreme warm summers and heatwaves over europe. Geophys. Res. Lett. 48, e2020GL091197 (2021).
- Fischer, E. M. et al. Storylines for unprecedented heatwaves based on ensemble boosting. Nat. Commun. 14, 4643 (2023).

- Yiou, P. & Jezequel, A. Simulation of extreme heat waves with empirical importance sampling. Geosci. Model Dev. 13, 763–781 (2020).
- 145. Kelder, T. et al. An open workflow to gain insights about low-likelihood high-impact weather events from initialized predictions. *Meteorol. Appl.* **29**, e2065 (2022).
- Cadiou, C. & Yiou, P. Simulating record-shattering cold winters of the beginning of the 21st century in France. EGUsphere 2024, 1–21 (2024).
- 147. Sippel, S. et al. Could an extremely cold central European winter such as 1963 happen again despite climate change? Weather Clim. Dyn. 5, 943–957 (2024).
- Thompson, V. et al. High risk of unprecedented UK rainfall in the current climate. Nat. Commun. 8, 107 (2017).
- Thompson, V. et al. Risk and dynamics of unprecedented hot months in South East China. Clim. Dyn. 52, 2585–2596 (2019).
- 150. Kelder, T. et al. Using unseen trends to detect decadal changes in 100-year precipitation extremes. npj Clim. Atmos. Sci. 3, 47 (2020).
- Ragone, F., Wouters, J. & Bouchet, F. Computation of extreme heat waves in climate models using a large deviation algorithm. Proc. Natl Acad. Sci. USA 115, 24-29 (2018).
- Gessner, C., Fischer, E. M., Beyerle, U. & Knutti, R. Very rare heat extremes: quantifying and understanding using ensemble reinitialization. J. Clim. 34, 6619–6634 (2021).
- Goulart, H. M. et al. Compound flood impacts from Hurricane Sandy on New York City in climate-driven storylines. Nat. Hazards Earth Syst. Sci. 24, 29–45 (2024).
- 154. Heinze-Deml, C., Sippel, S., Pendergrass, A. G., Lehner, F. & Meinshausen, N. Latent Linear Adjustment Autoencoders v1.0: a novel method for estimating and emulating dynamic precipitation at high resolution. Geosci. Model Dev. Discuss. 2020, 1–39 (2020).
- Huser, R. & Wadsworth, J. L. Advances in statistical modeling of spatial extremes. Wiley Interdiscip. Rev. Comput. Stat. 14, e1537 (2022).
- 156. Huser, R., Opitz, T. & Wadsworth, J. L. Modeling of spatial extremes in environmental data science: time to move away from max-stable processes. *Environ. Data Sci.* 4, 1–16 (2025).
- Zhong, P., Huser, R. & Opitz, T. Modeling nonstationary temperature maxima based on extremal dependence changing with event magnitude. *Ann. Appl. Stat.* 16, 272–299 (2022).
- Zhong, P., Brunner, M., Opitz, T. & Huser, R. Spatial modeling and future projection of extreme precipitation extents. J. Am. Statist. Assoc. 120, 80–95 (2024).
- Kelder, T. et al. How to stop being surprised by unprecedented weather. Nat. Commun. 16, 2382 (2025).
- Hersbach, H. et al. The ERA5 global reanalysis. Q. J. R. Meteorol. Soc. 146, 1999–2049 (2020).
- Fetterer, F., Knowles, K., Meier, W., Savoie, M. & Windnagel, A. Sea ice index, version 3. National Snow and Ice Data Center (2017).

Acknowledgements

E.M.F. and S.S. gratefully acknowledge funding from the EU Horizon 2020 Project XAIDA (grant agreement 101003469). M.B. and this project have received funding from the European Union's Horizon 2020 research and innovation programme under the Marie Sklodowska-Curie Grant agreement No. 101027577. R.H. was supported by the King Abdullah University of Science and Technology (KAUST) Office of Sponsored Research (OSR) under Award No. OSR-CRG2020-4394 and by his baseline research funds. E.J.K. was supported by the Met Office Hadley Centre Climate Programme funded by DSIT. S.S. acknowledges the climXtreme project funded by the German Federal Ministry of Education and Research (Phase 2, project PATTETA, Grant No. 01LP2323C) and the project 'Artificial intelligence for enhanced representation of processes and extremes in Earth system models' (AI4PEX; Grant agreement No. 101137682, funded by the EU's Horizon Europe programme). A.R. received funding from the European Union (ERC, FORCLIMA, 101044247).

Competing interests

The authors declare no competing interests.

Additional information

Supplementary information The online version contains supplementary material available at https://doi.org/10.1038/s43017-025-00681-y.

Publisher's note Springer Nature remains neutral with regard to jurisdictional claims in published maps and institutional affiliations.

Springer Nature or its licensor (e.g. a society or other partner) holds exclusive rights to this article under a publishing agreement with the author(s) or other rightsholder(s); author self-archiving of the accepted manuscript version of this article is solely governed by the terms of such publishing agreement and applicable law.

© Springer Nature Limited 2025